



HAL
open science

Structural Evolution and Formation of High-Pressure Plasmas in X Pinches

Jeremy P. Chittenden, Andrea Ciardi, C. A. Jennings, Sergey V. Lebedev, D. A. Hammer, S. A. Pikuz, T. A. Shelkovenko

► **To cite this version:**

Jeremy P. Chittenden, Andrea Ciardi, C. A. Jennings, Sergey V. Lebedev, D. A. Hammer, et al.. Structural Evolution and Formation of High-Pressure Plasmas in X Pinches. *Physical Review Letters*, 2007, 98, pp.25003. 10.1103/PhysRevLett.98.025003 . hal-03732538

HAL Id: hal-03732538

<https://hal.science/hal-03732538>

Submitted on 30 Jul 2022

HAL is a multi-disciplinary open access archive for the deposit and dissemination of scientific research documents, whether they are published or not. The documents may come from teaching and research institutions in France or abroad, or from public or private research centers.

L'archive ouverte pluridisciplinaire **HAL**, est destinée au dépôt et à la diffusion de documents scientifiques de niveau recherche, publiés ou non, émanant des établissements d'enseignement et de recherche français ou étrangers, des laboratoires publics ou privés.

Structural Evolution and Formation of High-Pressure Plasmas in X Pinches

J. P. Chittenden,¹ A. Ciardi,² C. A. Jennings,³ S. V. Lebedev,¹ D. A. Hammer,⁴ S. A. Pikuz,⁴ and T. A. Shelkovenko⁴

¹*Blackett Laboratory, Imperial College, London SW7 2BW, United Kingdom*

²*Observatoire de Paris, (LUTH), 92195 Meudon, France*

³*Sandia National Laboratory, Albuquerque, New Mexico 87185, USA*

⁴*Laboratory of Plasma Studies, Cornell University, Ithaca, New York 14853, USA*

(Received 19 July 2006; published 9 January 2007)

Two- and three-dimensional MHD simulations are used to provide a theoretical description of 2 wire molybdenum X -pinch experiments. The initial evolution from solid wires to the formation of supersonic jets and a central micro- Z pinch is found to result from the slow rate of wire ablation and from the distribution of the Lorentz force. The growth of $m = 0$ instabilities triggers the formation of micron sized regions of intense x-ray emission with plasma pressures in the Gbar range. A simple analytical model is used to predict how the maximum density and temperature scale with material and current.

DOI: [10.1103/PhysRevLett.98.025003](https://doi.org/10.1103/PhysRevLett.98.025003)

PACS numbers: 52.58.Lq, 52.65.Kj

X -pinch plasmas are formed when a fast rising current of a few hundred kA is applied to two or more thin metallic wires which are mounted so that they cross and touch at a single point in the form of an “ X ”. The magnetic field strength at the point where the wires cross is sufficiently strong to force a rapid compression of the wire material to form a transient high density and temperature plasma, which is an intense source of soft x rays. Initially, work on X pinches was concentrated upon their development as versatile laboratory radiographic tool [1–4]. The micron scale source size, the keV photon range and the short 10–100 ps burst duration make the X pinch an ideal source for point-projection radiography of rapidly evolving objects. As a consequence they have been extensively used to provide quantitative areal density measurements of wire array Z pinches [5] and other high density plasmas. Indeed, in experiments where two X pinches are used in parallel [6] the x-ray burst from one X pinch can be used to radiograph the second X pinch, revealing both plasma jet structures between the legs of the X pinch and a central micro- Z pinch (300–400 μm long) in which the micron sized point source is formed. More recently, fast streaked spectroscopy has revealed that this intense burst of x ray comes from a plasma with material densities close to solid and electron temperatures in the keV range [7,8]. In other words, it is possible, using university experiments of a modest scale, to produce materials of almost unprecedented thermal pressure and energy density.

In this Letter we describe a theoretical investigation of the three phases of X -pinch evolution. We use as an example, experiments on the XP pulser at Cornell University where a current rising to 460 kA in 40 ns was used to drive two X pinches, each comprised of two 17 μm molybdenum wires [6]. Using the GORGON [9] 3D resistive magnetohydrodynamics (MHD) code we show how the formation of plasma jets and the structure of the micro- Z pinch result from the magnetic field topology and the slow rate of wire ablation. Higher resolution simulations of the micro- Z pinch then show how the axial transport of mass resulting

from the $m = 0$ instability combined with strong radiative losses produce a micron sized high intensity source whose parameters are consistent with experimental observations. These results are then consistent with a simple model of a Z pinch in pressure and energy balance in the presence of axial mass loss, which allows an examination of how the peak densities and temperatures vary with current and material.

As with other pinches formed from metallic wires, the flow of current generates a low density plasma, or “corona”, on the surface of the wires early in time, with the majority of the mass remaining in a cold, dense, wire core. Since the core is highly resistive, the vast majority of the current flows in the surface corona and therefore the rate of energy deposition into the core is very slow and so is its ablation rate [5,9]. To model this system we use the 3D MHD code GORGON, using a similar setup to that described in Ref. [9]. For this application we use a Cartesian grid of 10 μm cubic cells which models the central 1.5 mm of the X pinch. Figure 1(a) shows the magnetic field topology after 10 ns. By this stage the wire cores (shown in gray) have expanded to $\sim 100 \mu\text{m}$ but still contain the vast majority of the mass. Here the magnetic topology results from the superposition of a local field component due to the current flowing in each wire and the global component generated by the total current, which is centered on the axis of the X pinch. The color contours in Fig. 1(a) show that far away from the cross point the local field dominates. On each wire, the field direction reverses from one side of the wire to the other and there is a field null ($B = 0$, in green) located near the wire core. Nearer the cross point, however, the wires are too close to allow field reversal to occur between the wires, the global field dominates and the only field null lies on the axis of the X pinch. The $j \times B$ vectors in Fig. 1(a) therefore show that far away from the cross point the plasma is in part pinched towards the center of each wire, but within $\pm 300 \mu\text{m}$ of the cross point, the plasma is accelerated only towards the central axis of the X pinch. The subsequent evolution of the

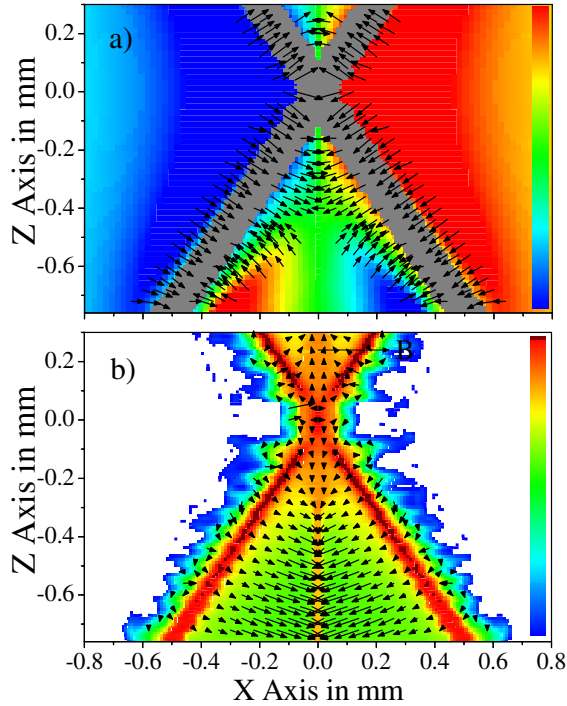


FIG. 1 (color online). Slices through the plane of the wires, showing (a) contours of B_y from -10 (blue) to 10 T (red) and vectors of $j \times B$ at 10 ns, (b) mass density contours from 10^{-4} (blue) to 10^3 kg/m^3 (red), and vectors of velocity at 26 ns.

plasma is predetermined by this magnetic topology, with the length of the micro-Z pinch being approximately given by the positions of the field nulls earlier in time.

In practice, the field reversal around the wires is not sufficient to prevent the coronal plasma from flowing in a direction perpendicular to the wires. Further ablation of the wire cores continuously replenishes the corona as it is removed, resulting in a steady stream of plasma arriving on the central axis [see Fig. 1(b)]. Since the flows are moving perpendicular to the wires, however, they retain an axial momentum which is conserved when the streams collide and thus two axial jets are formed propagating away from the cross-point at around 10^5 m/s. A strong radiative cooling rate means that the thermal energy gained by the two flows stagnating on one another is rapidly lost and the temperature remains low. Thus the jets have a high Mach number and low divergence and are similar to jets formed in conical wire array Z pinches [10,11].

The rate of wire core ablation is determined by the global magnetic field strength [12] and is thus a strong function of the axial position. Figure 1(b) shows that by 26 ns the wires cores within ± 120 μm of the cross point are full ablated and that this region has begun to implode towards the central axis.

This zippered implosion tends to result in an axial pressure gradient ($\partial P/\partial z$) which produces a flow of material away from the cross-point. In addition, as the cross point begins to collapse, the current flows axially along this collapsing Z pinch but then radially across the ends of the

cylinder, resulting in a $j_r B_\theta$ force which accelerates material axially, away from the cross point. By 28 ns this axial flow has depleted the mass per unit length of the collapsing Z pinch to 20% of its original value, transporting the mass to form two disklike plasma electrodes at ± 150 μm (see Fig. 2). The velocity vectors in Fig. 1(b) show that each central plasma jet has both a wide region within ~ 300 μm of the cross point (comprised of material transported by the axial $\partial P/\partial z$ and $j_r B_\theta$ forces) followed by a thinner jet region formed by the plasma flow perpendicular to the wires.

Figure 2 shows the structure just before, during and just after peak compression and comparisons of synthetic radiographs (areal density maps) with experimental data [6]. As time progresses a longer length of the wire core ablates and compresses to the axis and this combined with the axial $j_r B_\theta$ force serves to elongate the cylindrical micro-Z pinch that forms at the cross point. The combination of radiative cooling and axial mass loss, however, means that this pinch rapidly collapses to small size. The mass per unit length of the micro-Z pinch is smallest where the axial $j_r B_\theta$ force is largest, i.e., at the ends of the Z pinch and, consequently, in a simulation without any perturbation, we obtain two tightly compressing regions at the ends of the micro-Z pinch, with an isolated island of plasma at the center. By 30 ns, parts of the micro-Z pinch have collapsed below the resolution of the 10 μm simulation. The evolution of the rest of the X pinch, however, is still consistent with experiment. Late in time, the axial $j_r B_\theta$ force drives a strong shock into the plasma electrode structures. Since the magnetic field is largest on axis, the center of the electrode reaches higher velocity than the edges producing a characteristic quasispherical shock wave as observed in experiment [6].

To model the formation of the micron sized x-ray source requires higher resolution than the 10 μm used in the 3D calculations. Fortunately, the simulation results and the experimental radiographs indicate that the micro-Z pinch has good azimuthal symmetry. We therefore model the collapse using a cylindrical 2D(r, z) MHD simulation which solves the same equations as the 3D code but has a radial resolution varying from 5 μm at the outer edge down to 50 nm on axis and with a fixed 1 μm axial resolution. Figure 3 shows the mass density contours from a 2D(r, z) simulation of a 300 μm long micro-Z pinch initialized at 28 ns with 20% of the initial mass and a radius of 100 μm as predicted by the 3D code. A long wavelength (200 μm) harmonic velocity perturbation is introduced to initiate an $m = 0$ instability eigenmode and produce a single neck.

Normally, in high density Z pinches, the neck of an $m = 0$ instability will undergo a radiative collapse, where strong radiative cooling prevents the build up of thermal pressure and allows the magnetic field to continue compression. At these densities however the plasma starts to become optically thick and radiates like a blackbody (which sets an upper limit to the loss rate in the codes). The plasma then

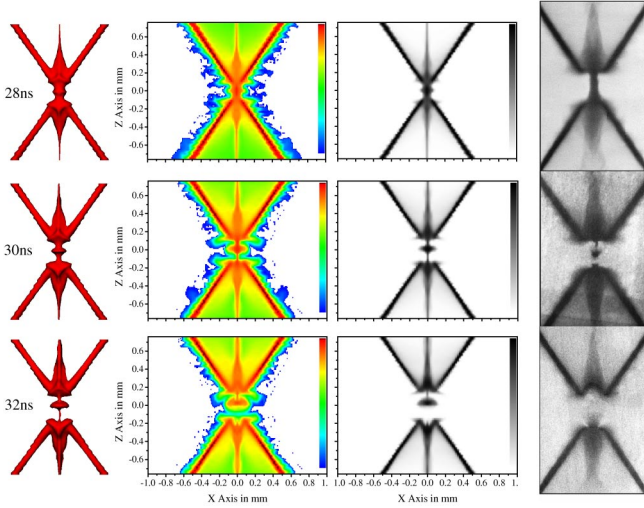


FIG. 2 (color online). 3D surfaces of constant density (1 kg/m^3), mass density contours in the plane of the wires, synthetic and experimental [6] radiographs.

approaches an equilibrium where the energy lost to black-body radiation is approximately balanced by Ohmic heating. This condition can be combined with the Bennett relation to derive the equilibrium radius and x-ray power [9].

$$r = 2.3 \times 10^{-18} I^{-14/9} \beta^{-4/3} f^{13/9} N^{10/9} \ln \Lambda^{1/3} \quad (\text{m}), \quad (1)$$

$$P = 6.7 \times 10^{22} I^{34/9} \beta^{8/3} f^{-11/9} N^{-14/9} \ln \Lambda^{1/3} \quad (\text{W m}^{-1}), \quad (2)$$

where N is the ion line density (ions per meter), $\ln \Lambda$ is the Coulomb logarithm, β is the ratio between the radiation and electron temperatures (here $\beta \sim 1$), and f comes from an approximate form for the ionization level; $Z^* \sim f T_e^{1/2}$. For molybdenum, we choose $f = 2$ and $\ln \Lambda = 5$. Since over the time scale of the collapse, the current (I) is essentially constant, the principle parameter determining the plasma radius is the ion line density. In both 3D and 2D calculations, the plasma at the center of the micro- Z pinch is in approximate pressure and energy balance. It is the $\partial P / \partial z$ and, more importantly, the $j_r B_\theta$ force which then determine the rate of axial mass transport away from the neck region and thus determine the radius of the collapsing plasma.

In the long wavelength case shown in Fig. 3, once the length of the neck region becomes long compared to its radius, both the $\partial P / \partial z$ and the $j_r B_\theta$ forces are large at the ends of the neck region and negligible at the center. Mass depletion at the center therefore ceases and this region stops collapsing. The ends of the neck region start to form two identical, smaller, collapsing necks. This “bifurcation” [13] or “cascading” [14] of the neck regions continues until 8 or 16 necks are formed, depending on the resolution. In experiments, such a symmetric perturbation will not occur, so while this process may explain why

multiple x-ray bursts are often observed [6], the bifurcation process is unlikely to repeat itself to the extent seen in simulation.

If a more localized, v -shaped, short wavelength ($50 \mu\text{m}$) perturbation is applied, the neck remains short and does not bifurcate, allowing the plasma parameters to be followed at a single point, throughout a continuous implosion. In all of these calculations the axial flow velocity away from the neck is given roughly by the local sound speed. Under these conditions we can write a simple form for the time dependence of the ion line density and therefore solve Eq. (1) and the Bennett relation nonlinearly to obtain the average plasma parameters as functions of time and to compare them to the results of the short wavelength 2D simulation.

Since the line density asymptotically approaches zero at some characteristic “opening time”; Fig. 4 plots the plasma parameters from the two models as functions of the time left before opening. This then gives characteristic time scales for the different sets of plasma conditions. For this example, the nonlinear solution of Eq. (1) provides a fair representation of the collapse region as modeled by the 2D code. Equation (1) predicts that as the line density tends to zero, the plasma in the collapse region approaches zero radius and infinite density. A number of physical processes will prevent the plasma from reaching this point. One such effect occurs, in this example, when the line density of the plasma drops below $\sim 0.2\%$ of the original value. Beyond this point we would expect the drift velocity of electrons to exceed the ion sound speed, a condition which initiates the growth of microinstabilities and results in resistivity values far in excess of the Spitzer value. This produces a substantial increase in Ohmic heating, which causes an explosion of the micro- Z pinch and thus terminates the collapse. By using the Bennett relation, the condition of drift velocity equal to sound speed can be used to derive a critical line density $N = 1.3 \times 10^{18} A / Z^{*2} \text{ (m}^{-1}\text{)}$. Assuming $Z^* \sim Z \sim A/2$, this yields a unique mass per unit length of $\sim 8 \times 10^{-9} \text{ kg/m}$, which represents a limit to the collapse process. This point is indicated in Fig. 4 by blue squares. To see the effect of this limit in MHD simulations an anomalous resistivity term based upon the lower-hybrid drift microinstability [15] was introduced into the 2D code. The red line in Fig. 4 then shows that

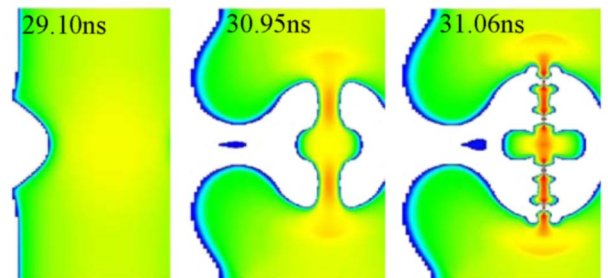


FIG. 3 (color online). Mass density contours from 2D(r, z) simulation of $m = 0$ in micro- Z pinch.

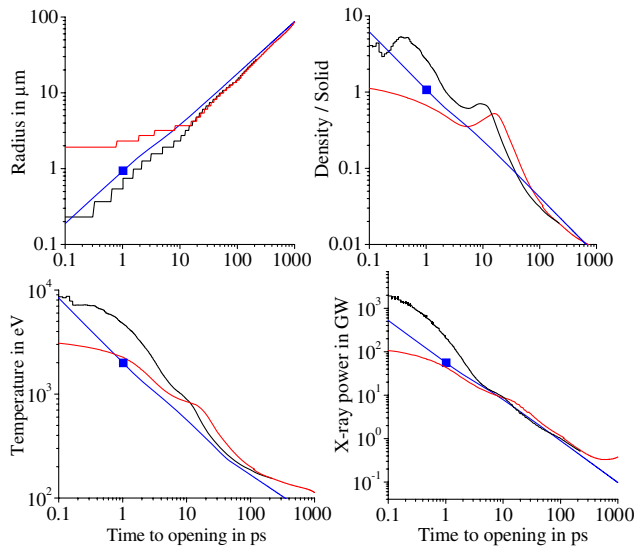


FIG. 4 (color online). Radius, peak density, temperature, and radiation output of the collapse region versus time before opening, from Eq. (1) (blue), 2D simulation (black), and 2D simulation with anomalous resistivity (red).

collapse follows the previous result before undergoing a spontaneous termination at around the point when the mass per unit length in the neck falls below 8×10^{-9} kg/m.

In order to compare these data to experimental observations it is important to note that the plasma parameters determined from experiments are dependent on the temporal resolution and wavelength range of the instrument. There is, however, a clear trend in the experimental measurements towards smaller source sizes and shorter x-ray bursts as the wavelength at which the observation is made decreases. This is entirely consistent with the theoretical model of an $m = 0$ neck where axial mass transport allows the temperature to rise as the radius decreases. The recent results using fast streaked soft x-ray spectroscopy [7,8] have now revealed the plasma parameters close to peak compression. If the anomalous resistivity provides the mechanism to terminate collapse, then both models predict that at peak compression the plasma has collapsed to a micron in diameter and has reached solid density, the temperature is 2 keV the output power is 5 GW and the lifetime is 2 ps. These five parameters are then consistent with the faster time scale diagnostic results presented in Refs. [7,8].

The minimum mass per unit length provides an estimate for the peak compression that can be obtained which

appears to be adequate for the present 100 kA class machines. For example, the minimum radius scaling as $r \sim I^{-14/9} Z^{-10/9}$ suggests that in order to reach a radius of less than $1 \mu\text{m}$ requires a current of 100 kA for molybdenum, 516 kA for aluminum, but only 45 kA for tungsten, which is roughly consistent with experiments at Cornell University [6–8], at Pontificia Universidad Católica de Chile [16], and at Imperial College [17]. Scaling the driver current up to 1 MA however, the strong radius ($I^{-14/9}$) and density scaling ($I^{28/9}$) suggest a 30 nm sized object at 1290 times solid density. It seems more likely that other processes such as a lack of azimuthal symmetry will terminate the collapse before reaching the minimum mass per unit length. If instead we assume that the symmetry of convergence places a lower limit on the radius of $1 \mu\text{m}$, then Eqs. (1) and (2) suggest an 80 GW molybdenum source at 10 times solid density can be achieved using a 1 MA drive current and a 3.4 TW source at 250 times solid density at 10 MA. These results suggest that the phenomenon of radiative collapse in X-pinch plasmas can potentially be extrapolated to produce material under extremes of pressure and density far higher than those already achieved. It remains to be seen whether sufficient symmetry can be retained during implosion to reach such plasma conditions.

This work was supported by the EPSRC and by the U. S. Department of Energy through cooperative agreement No. DE-FC03-02NA00057.

-
- [1] S. M. Zakharov *et al.*, Sov. Tech. Phys. Lett. **8**, 456 (1982).
 - [2] D. A. Hammer *et al.*, Appl. Phys. Lett. **57**, 2083 (1990).
 - [3] D. Kalantar *et al.*, Rev. Sci. Instrum. **66**, 779 (1995).
 - [4] S. A. Pikuz *et al.*, J. Quant. Spectrosc. Radiat. Transfer **51**, 291 (1994).
 - [5] S. V. Lebedev *et al.*, Phys. Rev. Lett. **85**, 98 (2000).
 - [6] T. A. Shelkovenko *et al.*, Phys. Plasmas **8**, 1305 (2001).
 - [7] T. A. Shelkovenko *et al.*, Phys. Plasmas **9**, 2165 (2002).
 - [8] S. A. Pikuz *et al.*, Phys. Rev. Lett. **89**, 035003 (2002).
 - [9] J. P. Chittenden *et al.*, Plasma Phys. Controlled Fusion **46**, B457 (2004).
 - [10] S. V. Lebedev *et al.*, Astrophys. J. **564**, 113 (2002).
 - [11] A. Ciardi *et al.*, Laser Part. Beams **20**, 255 (2002).
 - [12] S. V. Lebedev, Phys. Plasmas **8**, 3734 (2001).
 - [13] J. P. Chittenden *et al.*, Phys. Plasmas **4**, 2967 (1997).
 - [14] G. V. Ivanenkov *et al.*, JETP **91**, 469 (2000).
 - [15] J. P. Chittenden *et al.*, Phys. Plasmas **2**, 1242 (1995).
 - [16] I. H. Mitchell *et al.*, Phys. Plasmas **7**, 5140 (2000).
 - [17] F. N. Beg *et al.*, Appl. Phys. Lett. **82**, 4602 (2003).